VALIDATION OF A METHOD FOR SNOW COVER EXTENT MONITORING OVER QUEBEC (CANADA) USING NOAA-AVHRR DATA

Karem Chokmani[1], Monique Bernier[1] and Michel Slivitzky[2]

1. INRS-ETE, 490 rue de la Couronne, CP 7500, Québec (Qc), Canada G1K 9A9; {karem.chokmani / monique.bernier}(at)ete.inrs.ca
2. Ouranos, 550 rue Sherbrooke Ouest, Montréal (Québec), Canada H3A 1B9; slivitz(at)cite.net

ABSTRACT

This work comes within the scope of a multidisciplinary study aimed at validating the hydrological simulations of the Canadian regional climate model over Quebec (Canada). Snow cover is a key factor in the modelling process. Because of their low density, conventional local observation networks do not provide enough accurate data to map snow cover on a large scale and with an adequate spatial resolution for regional climate modelling. Alternatively, this is easily feasible using visible and infrared satellite imagery. However, available satellite snow cover products are unusable for our special needs, because they either have an inadequate spatial resolution or too short observation series.

The objective of this study was therefore to develop an automatic algorithm for snow cover extent mapping using data from the AVHRR sensor on board NOAA satellite series, which allows monitoring the space-time evolution of snow cover extent over a long period of time and with a "fine" spatial resolution (1x1 km^2). Snow cover extent mapping results were validated against in situ snow occurrence observations. The algorithm was tested over the province of Quebec (Canada) for three specific periods: 1998-1999, 1991-1992 and 1986-1987. The algorithm identifies surface class (snow/no-snow) with an average total success rate of 87%. The algorithm performances were higher in snow detection (90%) than they were for no-snow surfaces (82%).

Keywords: Snow cover extent, AVHRR, threshold algorithm

INTRODUCTION

This work lies within the scope of a multidisciplinary study aiming at validating the elements of the hydrological cycle of the Canadian regional climate model simulations (CRCM) over Quebec (Canada) (1). These simulations, carried out over a 20 years' period (1979-1999), aim at examining the annual and inter-annual hydrological budget on a dozen of catchments. Snow cover is a key factor in the modelling process of the hydrological budget as well as of the climatic changes. The remote sensing component of the project is interested in exploiting the satellite data in order to validate CRCM simulations of the snow cover characteristics (i.e. snow cover extent), which are impossible to validate using the conventional *in situ* snow observations.

Satellite data in the visible and the infra-red spectrum as well as in the passive microwaves represent an alternative source of information on snow cover. Various satellite snow products have been available since the middle of the 1960's and for some they are available in real time and online (2). However, their quality varies considerably according to the sensor and the platform characteristics, to image processing procedures and to snow classification techniques (3). Consequently, these operational products cannot be used for the validation of the CRCM simulations because of the limited spatial extent for some, of the coarse spatial resolution for others and/or of the non-availability of a continuous and homogeneous series of observations covering the targeted period (1979-1999). For example, the snow maps produced by National Operational Hydrological Remote Sensing Center (NOHRSC) (2), of a resolution of 1 km, have a limited space cover. Those produced by the National Environmental Satellite Data and Information Service (NESDIS) did reach a suitable resolution (<10 km) only after 1997 (4). As for the maps produced using MODIS

images (500 m), they have been available only since the end of 1999 (5). In addition, the coarse temporal resolution and the small extent of the scene of high-resolution satellites limit their use in the temporal monitoring of snow cover on a regional scale (5).

Consequently, it was decided to explore the potential of NOAA-AVHRR data for the space-time monitoring of snow on ground and to produce snow cover extent maps. In future study, these maps will be used to validate CRCM simulations. Among the 20 years concerned by the study (1979-1999), six winter seasons were appointed to be used in the validation process. Among them, three winters were selected for the exploration of the sensor potential and the development and validation of the initial approach, namely 1986-1987, 1991-1992 and 1998-1999.

DATA AND METHODS

At first, an automatic algorithm of snow mapping using AVHRR data was developed for the studied region while being based on the published methods and algorithms detailed hereafter. Then, the mapping results were validated using ground observations of snow occurrence.

Satellite data

The images come from the AVHRR sensor on board of the NOAA satellite series (6). In order to monitor the evolution of snow cover, especially during snow setting and melt phases, the daily images from 1 October to 15 December and from 1 April to 31 May of each of the three periods were used. The images at the beginning of the afternoon were privileged, since they are less sensitive to variations in topography and in illumination conditions effects. Only the images presenting a minimal cloud cover were retained (164 images out of the 411 initially identified). These selected images were used for calibration and validation of the snow cover extent mapping algorithm.

Rough AVHRR data were calibrated and radiometrically corrected. The calibration procedure takes into account the temporal variation of the calibration parameters of the sensor (7). Visible and near infra-red data (bands 1 and 2) were converted into albedo ($A1$ and $A2$). Mid and thermal infrared data (bands 3, 4 and 5) were converted into brightness temperatures ($T3$, $T4$ and $T5$). Bands 1 and 2 data were standardized according to the illumination conditions (solar zenith angle and Earth-Sun distance corrections). The images have not been corrected for atmospheric effects due to the lack of ancillary atmospheric data and to the difficulties in applying these corrections to an important data series. The images were corrected geometrically using satellite orbital data. Finally, a sub-region (82°30'W, 58°N; 60°W, 46°N) covering the territory studied was extracted from each image (Figure 1).

Snow mapping algorithm

Several techniques using visible and infra-red satellite data were applied successfully for snow mapping: supervised spectral classification (8), artificial neural networks (9), segmentation techniques (10) or sub-pixel modelling (11). However, these techniques are less effective on a regional or global scale, since they require an intensive effort for their calibration and their application. Consequently, for snow monitoring studies on a large scale and over a long period of time, classification approaches using hierarchical thresholds are more appropriate because of their simplicity, transparency and speed (12).

Various threshold algorithms applied to AVHRR imagery were proposed (13,14). The thresholds are based on the differences in the spectral response of terrestrial surfaces in the AVHRR bands. They are obtained empirically and differ from an algorithm to another. They are applied to the entire image pixel by pixel in a sequential way. The classification algorithm developed in the present study was inspired by that proposed by Voigt *et al.* (15). It is a threshold algorithm designed to distinguish three categories: snow, no-snow and clouds. It consists of a combination of 6 sequential thresholds. The thresholds go from the least restrictive to the most severe. A pixel which succeeds in passing through all the thresholds, is classified as snow, if it is not categorized either as clouds or no-snow (Figure 2).

All threshold algorithms employ reflectance in band 3 of AVHRR (3.7 µm) as separation criterion between snow and clouds. In fact, in band 3, snow-covered surfaces are characterized by a lower reflectance than low clouds made of water droplets. This is less true for the ice clouds. However, reflectance in band 3 is not directly available in AVHRR data. Kongas *et al.* (16) proposed to use the temperature difference $T3$-$T4$ as an estimate of band 3 reflectance. This latter method was applied in this study. Hence, the threshold using the band 3 reflectance is different from that proposed initially by Voigt *et al.* (15).

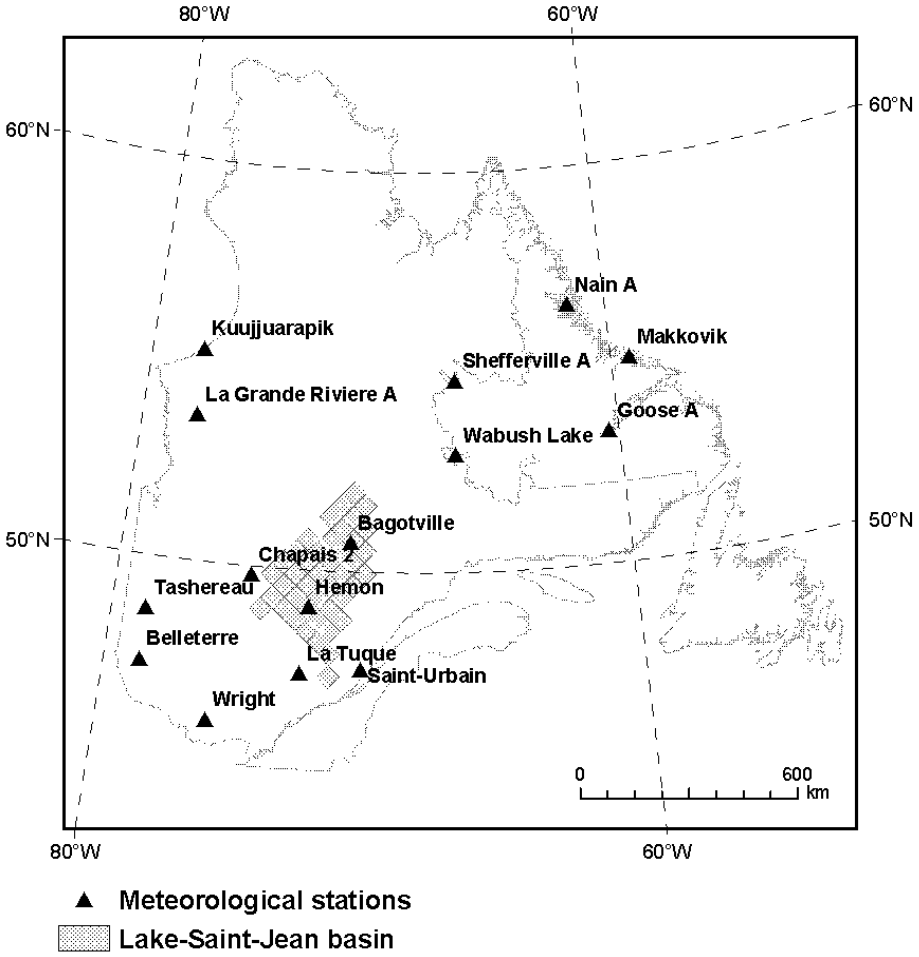

Figure 1: Extent of AVHRR sub-images and localization of the meteorological stations used in the temporal validation of the classification results.

To calibrate the algorithm, pixel samples were extracted from each selected image, above areas belonging to the three surface categories present within the scene. These areas were identified visually and delimited manually. Thereafter, radiometric data ($T4$, $\Delta T45$, *NDVI*, $\Delta T34$ and $A1$) of the samples from all selected images were put together and their percentiles were calculated. The percentiles were used to build the values of the algorithm thresholds. The value of a given threshold is fixed to the percentile that allows separating the snow pixel from the other classes.

For each period, two dates were chosen for the spatial validation of the snow map produced by the AVHRR: one during the snow cover setting period (at the end of October) and the other for the period of snow melt in spring (at the end of April). Moreover, these dates were selected because of the presence of the three surface categories as well as relatively weak cloud cover. For the six selected dates, ground snow occurrence recorded at a certain meteorological station operated by Environment Canada was compared to the results of AVHRR image classification. Ground snow occurrence was deduced from snow observations recorded at the meteorological stations (a station was considered snowfree when the snow depth value was nil). Also, snow occurrence observations at 15 meteorological stations during all three winter seasons were used for the temporal validation of the classification algorithm (Figure 1).

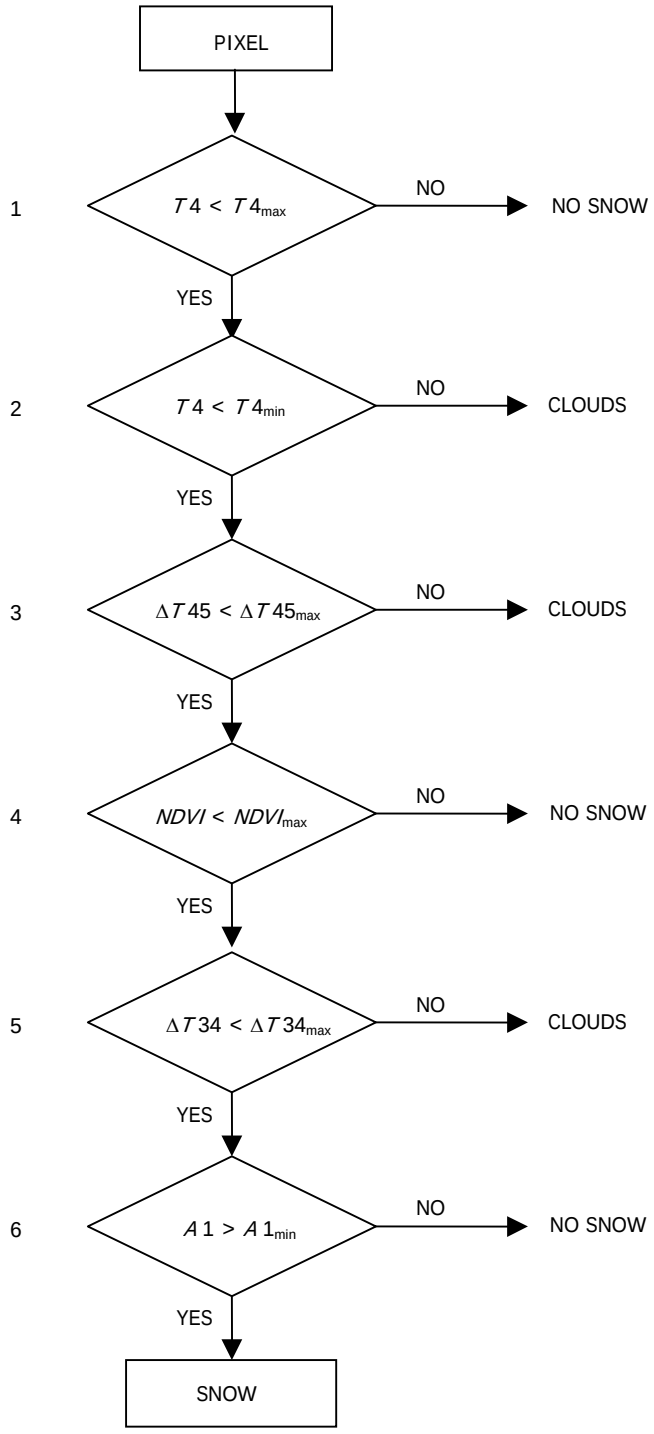

Figure 2: Flow chart of the sequential hierarchical classification algorithm of AVHRR images (inspired by Voigt et al. *(15)). To be identified as snow, a pixel must have a* T*4 value lower than the maximum snow temperature. If not, the pixel is classified as no-snow; the pixel must also have a* T*4 value higher than the minimal snow temperature could have. If not, the pixel is classified as clouds (usually colder than snow); the pixel must have a temperature difference (*T*4-*T*5) lower than that of cirrus cover. If not, the pixel is classified as clouds; the pixel must have an* NDVI *value lower than the maximum which snow could have. If not, the pixel is classified as no-snow; the pixel must also have a temperature difference (*T*3-*T*4) lower than the maximum value than snow could have. If not, the pixel is classified as clouds; and the pixel must have a value of reflectance* A*1 higher than the minimal snow value. If not, the pixel is classified as no-snow.*

Ground observations corresponding to images acquisition time were compared to the occurrence of snow class within 3x3 pixels windows centred on each station. The total success rates of the classification, the omission and commission errors (matrix of confusion) and the respective values of the Kappa coefficient *K* were therefore calculated. When 50% or more of the 3x3 pixels windows was identified by the algorithm as cloudy, the results for the corresponding station were excluded from the comparison.

RESULTS

Comparison tests (Student test) carried out on the data extracted above the sampling areas showed that the radiometric characteristics of the various surface categories differ significantly depending on whether it is a matter of autumn or spring images. Consequently, we built two versions of the algorithm: one for autumn and another for spring.

The first and the second thresholds correspond ($T4$) to the 99th and the 1st percentile, respectively of the $T4$ temperature observed above the samples of snow-covered pixels. It should be noted that temperature values are higher in spring than they are in autumn. This reflects the mild conditions during the snow melt period. The third threshold ($\Delta T45$) value, however, is temporally stable. The value of this threshold was established at 2°K, a typical value used to detect the majority of the thin cloudy veils. As for the fourth threshold (*NDVI*), its value corresponds to the 99th percentile of *NDVI* of pixels belonging to snow class. The fifth threshold ($\Delta T34$) represents the principal discriminant between snow and cloud classes. However, this threshold does not make it possible to precisely separate between snow-covered surfaces and ice clouds, which are more frequent towards the end of the autumn. For this reason, the value of this threshold was fixed for the autumn period at a more severe level: 95th percentile against the 99th percentile for the spring images. The value of the sixth threshold ($A1$) being used to separate snow from no-snow pixels was established at the 1st percentile of the albedo in band 1. This is based on the fact that the pixels without snow have a reflectance level in band 1 lower than that of the snow-covered pixels. Table 1 presents the threshold values thus obtained.

Table 1: Thresholds of the AVHRR images used in the classification algorithm.

Threshold	Parameter	Autumn	Spring
1	$T4_{max}$	274.9 K	289.3 K
2	$T4_{min}$	240.2 K	254.2 K
3	$\Delta T45_{max}$	2 K	2 K
4	$NDVI_{max}$	0.14	0.19
5	$\Delta T34_{max}$	7.4 K	11,3 K
6	$A1_{min}$	22.8%	12.1%

Figure 3 shows the extent of the snow cover produced for each of the three studied periods and for each of the two appointed dates. In spite of the presence of clouds during the six dates, it is possible to clearly distinguish the snow front-line. Thus, by comparison with the snow extent during the 1998-1999 season, which represents an average year according to the winter season length, the 1986-1987 winter season was shorter. It seems that in 1987 snow melting started much earlier than in 1999. Indeed, although the snow front-line was on the same level in October 1987 and 1998, the snow front-line was much more to the north at the end of April 1987 than it was in 1999. As for the 1991-1992 period, the winter season shifted as compared to the 1998-1999 season: snow cover was established later in autumn and disappeared later in spring. Thus, at the end of October 1991, the snow front-line was still far in the north. At the end of April 1992, areas that should normally be snow-free in this period of the year were still covered with snow.

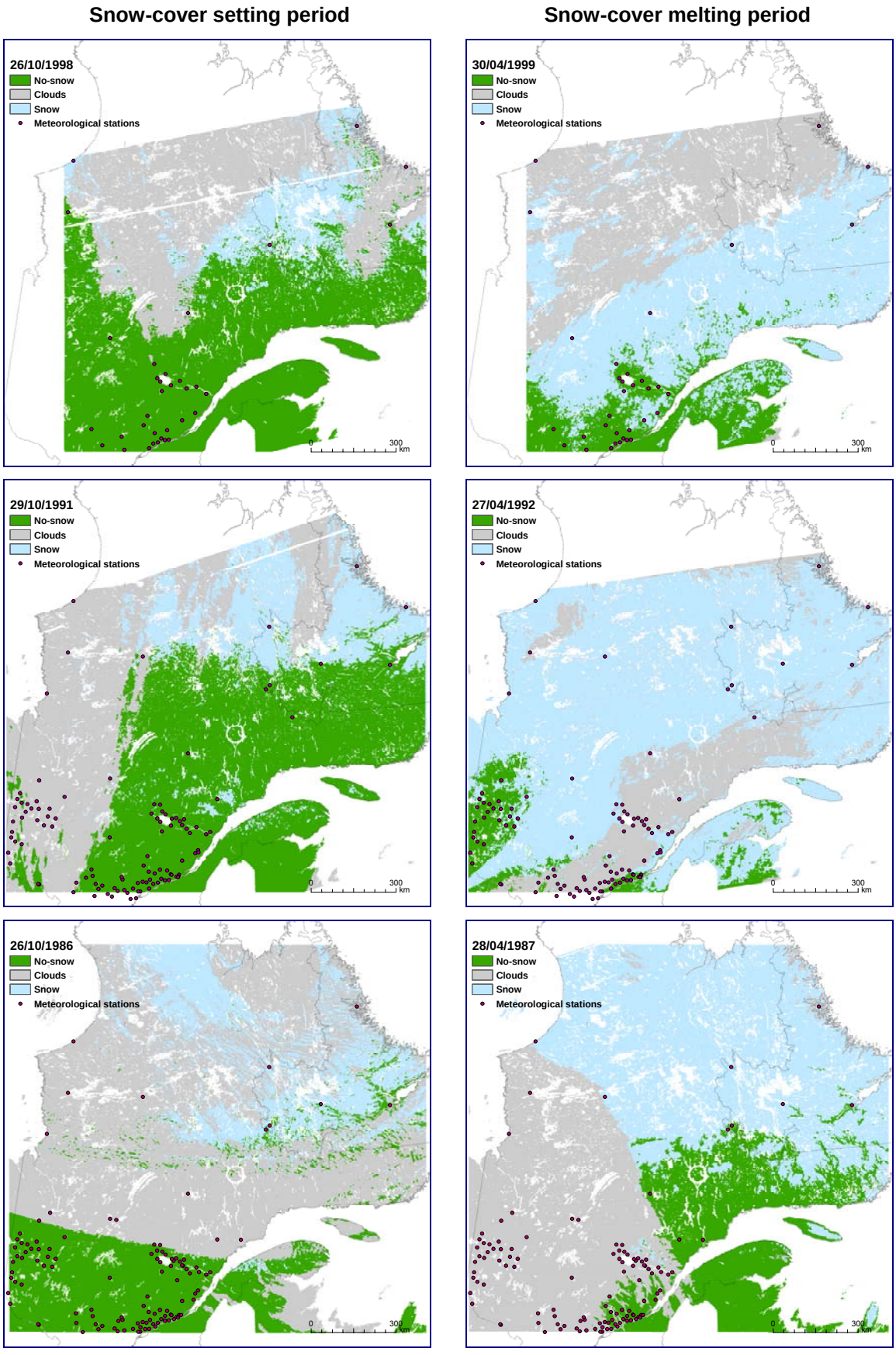

Figure 3: Snow cover extent maps obtained using the 6 AVHRR images selected during the snow setting and melting periods (blank lines in October's 1998 and 1991 maps are due to missing lines in AVHRR images).

Visual examination of the snow mapping results for the six dates appointed for the spatial validation (Figure 3) shows the capacity of the algorithm to reproduce the spatial variability of snow and no-snow surface categories as well as its capability to seize the inter-annual differences between the three seasons studied. However, careful examination of Figure 3 shows that the algorithm generates a certain confusion between snow and clouds. This appears clearly for example in the April 27, 1992 map: in the extreme south-west of the territory, a cloudy band was confused with snow. The examination of the mapping results of all dates (not presented here) shows that in spite of the use of the fifth threshold (dedicated to the distinction between clouds and snow) the algorithm identifies high clouds as snow. Generally, these clouds are made of ice crystals. Also, if there are two layers of superimposed clouds, the shade which the upper layer throws on the lower one is in certain cases classified wrongly as snow. It was proven that the difference in temperature ($T3$-$T4$) for shaded clouds is lower than the value selected of the fifth threshold particularly in spring (which is less severe than the value for autumn period) (Table 1). This means that the value of this threshold should be diminished in order to take account of these particular cases.

Table 2 compares results between the ground snow observations corresponding to the acquisition dates and the occurrence of the snow class inside the 3x3 pixels windows centred on each meteorological station retained for the spatial validation. The number of meteorological stations varies from one period to another.

According to classification results (Table 2), the algorithm correctly identified the surface class around meteorological stations with success rate of 73% in the worst case and 97% in the best case in the absence of clouds. This corresponds to a classification quality going from acceptable (K=0.44) to very good (K=0.87). However, certain sites under snow cover were incorrectly classified with an omission error sometimes exceeding 60%. This is explained by the relatively low number of sites under snow cover available for the analysis compared to the number of sites belonging to the snow-free category.

It should be noted that the results obtained for the six selected dates (Table 2) are biased even if they were calculated using a high number of meteorological stations. Indeed, most of these stations were located in the south-western part of the territory while only few stations were available in the north and the north-west (Figure 3). This artificially favours the classification results for the no-snow category to the detriment of the snow class, since the latter was underrepresented in the reference data set.

Table 3 presents the classification results compared with snow observations at the 15 temporal validation stations illustrated in Figure 1. For all stations, approximately 50% of the dates were contaminated by clouds, and this was more important in autumn. For the remaining dates, the classification algorithm correctly identified the surface conditions around all stations in 87% of the cases. This corresponds to a very good classification quality (K=0.72). It should be noted that the classification results of the snow class agree very well with the ground observations with a success rate for this class of about 90%. On the other hand, the performances of the algorithm to identify the no-snow class are weaker. These results show a slight tendency of the algorithm to underestimate the presence of the no-snow class. This was more important for the snow melting period where the no-snow class was correctly identified with a success rate of 79% compared to 86% during the autumn period. The tendency of the algorithm to underestimate the no-snow class is explained by the fact that snow is more metamorphosed (denser and with larger grain size) in spring than at the beginning of the winter season (fresh snow, fine grains). It results in a decrease of the snow reflectance increasing, by the way, the risk of confusion with surfaces without snow. This appears clearly in the value of the sixth threshold of the algorithm which does not differ from the value of the 1st percentile of snow reflectance in the red channel. This threshold responsible for separation between snow and no-snow is half a value lower in spring than in autumn (Table 1). Therefore, in order to increase the detection success rate of the no-snow category, it would be reasonable to raise the value of this threshold.

Table 2: Classification results of the six AVHRR images compared with snow observations at meteorological stations.

26 October 1998		Classification results					
		Snow	No snow	Cloud†	Total	Omission	Success
Ground observations	Snow	4	1		5	20%	80%
	No snow	0	28		28	0%	100%
	Cloud			1	1		
	Total	4	29	1	34		97%
Commission		0%	4%			Kappa=0.87	
30 April 1999		Classification results					
		Snow	No snow	Cloud†	Total	Omission	Success
Ground observations	Snow	7	2		9	22%	78%
	No snow	2	20		22	9%	91%
	Cloud			3	3		
	Total	9	22	3	34		87%
Commission		22%	10%			Kappa=0.69	
29 October 1991		Classification results					
		Snow	No snow	Cloud†	Total	Omission	Success
Ground observations	Snow	4	7		11	64%	36%
	No snow	0	64		64	0%	100%
	Cloud			28	28		
	Total	4	71	28	103		91%
Commission		0%	10%			Kappa=0.49	
27 April 1992		Classification results					
		Snow	No snow	Cloud†	Total	Omission	Success
Ground observations	Snow	18	6		24	25%	75%
	No snow	11	27		38	29%	71%
	Cloud			42	42		
	Total	29	33	42	104		73%
Commission		38%	18%			Kappa=0.44	
26 October 1986		Classification results					
		Snow	No snow	Cloud†	Total	Omission	Success
Ground observations	Snow	3	5		8	62%	38%
	No snow	1	94		95	1%	99%
	Cloud			14	14		
	Total	4	99	14	117		94%
Commission		25%	5%			Kappa=0.47	
28 April 1987		Classification results					
		Snow	No snow	Cloud†	Total	Omission	Success
Ground observations	Snow	3	0		3	0%	100%
	No snow	3	22		25	12%	88%
	Cloud			87	87		
	Total	6	22	87	115		89%
Commission		50%	0%			Kappa=0.61	

† : In the absence of ground observations on the cloud cover, the pixels classified as clouds were not included in success rates and Kappa coefficient calculation.

Table 3: Classification results of all retained AVHRR images compared with snow observations at 15 validation meteorological stations.

All dates: 1986, 1991 and 1998		Classification results					
		Snow	No snow	Cloud†	Total	Omission	Success
Ground observations	Snow	479	53		532	10%	90%
	No snow	57	255		312	18%	82%
	Cloud			960	960		
	Total	536	308	960	1804		87%
Commission		11%	17%			Kappa=0.72	
Autumns: 1986, 1991 and 1998		Classification results					
		Snow	No snow	Cloud†	Total	Omission	Success
Ground observations	Snow	169	19		188	10%	90%
	No snow	17	102		119	14%	86%
	Cloud			389	389		
	Total	186	121	389	696		88%
Commission		9%	16%			Kappa=0.75	
Springs: 1987, 1992 and 1999		Classification results					
		Snow	No snow	Cloud†	Total	Omission	Success
Ground observations	Snow	310	34		344	10%	90%
	No snow	40	153		193	21%	79%
	Cloud			571	571		
	Total	350	187	571	1108		86%
Commission		11%	18%			Kappa=0.70	

† : In the absence of ground observations on the cloud cover, pixels classified as clouds were not included in success rates and Kappa coefficient calculation.

Since the 15 meteorological stations employed for the temporal validation were uniformly distributed across the territory (Figure 1), their results must be used to characterize the performances of the algorithm developed and applied in the present work.

Hence, these results are comparable with those obtained in other studies using similar methods. Voigt *et al*. (15), for instance, found that the results of their approach applied to the Swiss territory agree with the observations on the ground in 86% of the cases. As for Romanov *et al*. (17), their threshold technique combining GOES (visible and infra-red sensor) and SSM/I (passive microwaves) data succeeded in mapping the snow cover extent over North America with a success rate of 85%. Also, Appel & Bach (18) developed and applied a threshold algorithm for snow detection over Germany using NOAA-AVHRR with a success rate of 95%.

Besides, due to the lack of cloud reference data, it was impossible to validate the classification results of clouds. Thus, the total success rate of the algorithm, which is 87% (Table 4), reflects only the performances of the algorithm according to snow and no-snow surface categories. If such validation data were available, this rate should be different from that illustrated in Table 4. The success rate will vary then according to the possible classification success rate of clouds: If clouds are well identified, the total success rate would be higher than or equal to the current rate; if not, the performances would be weaker.

The algorithm performances around the same 15 meteorological stations were also considered according to the land cover types (Table 4). The 15 meteorological stations were split into three land cover classes: forest, transition and open areas. The land cover types were derived from the land cover digital map of Canada produced by the Canadian Center of Remote Sensing which has a 1 km spatial resolution (19). As envisaged, the classification algorithm yields better results in open area than under forest. This is mainly due to the fact that the presence of a more or less

dense forest cover darkens more or less the snow-covered pixels and masks the subjacent snow. Consequently, the pixel is dominated by the spectral signature of forest to the detriment of snow which results in a higher classification precision of the snow class in open area (95%) compared to forest (89%). The algorithm shows intermediate performances in transition areas.

Table 4: Classification results of all retained AVHRR images compared with snow observations at 15 validation meteorological stations, according to land cover types.

Forest (8 sites) : 1986, 1991 and 1998		Classification results					
		Snow	No snow	Cloud†	Total	Omission	Success
Ground observations	Snow	194	25		219	11%	89%
	No snow	34	186		220	15%	85%
	Cloud			461	461		
	Total	228	211	461	900		87%
Commission		15%	12%			Kappa=0.73	
Transition (2 sites) : 1986, 1991 and 1998		Classification results					
		Snow	No snow	Cloud†	Total	Omission	Success
Ground observations	Snow	89	17		106	16%	84%
	No snow	3	41		44	7%	93%
	Cloud			131	131		
	Total	92	58	131	281		87%
Commission		3%	29%			Kappa=0.71	
Open area (5 sites) : 1987, 1992 and 1999		Classification results					
		Snow	No snow	Cloud†	Total	Omission	Success
Ground observations	Snow	196	11	0	207	5%	95%
	No snow	20	28	0	48	42%	58%
	Cloud	0	0	368	368		
	Total	216	39	368	623		88%
Commission		9%	28%			Kappa=0.57	

† : In the absence of ground observations on the cloud cover, pixels classified as clouds were not included in success rates and Kappa coefficient calculation.

The validation results according to land cover types agree with previously published results on the subject (5,20,21,22): snow detection is easier in open area than under forest, where trees mask the signal of subjacent snow. However, here too, the validation was affected by a slight bias. Indeed, the decreasing density gradient of the forest has a north-south direction which is practically the same for the increasing duration of the winter season. Consequently, in open areas, the no-snow class was underrepresented which would explain the lower classification success rate for this surface category (Table 4).

In addition, the classification results of AVHRR images were compiled on a dozen basins over the province of Quebec. We present here only those of the Lac-Saint-Jean basin (81,000 km^2) (Figure 1). The basin area was cut out on the simulation grid (45x45 km) of the CRCM. Figure 4 gives the percentage of the basin occupied by each of three surface categories (here, only the 1998-1999 season's results are presented). For certain dates, the image did not cover the whole area of the basin. Consequently, the sum of the percentages of the basin occupied by each of the three classes is lower than 100%. In spite of the presence of a rather important cloudy cover (particularly in the autumn images) it is possible to locate the dates of the beginning of the snow cover setting and melting periods over the basin (Figure 4). For example, on May 05, 1999, nearly 50% of the Lac-Saint-Jean basin was still covered with snow. These results thus showed the capacity of the classification algorithm to monitor the temporal evolution of the snow cover at the watershed level.

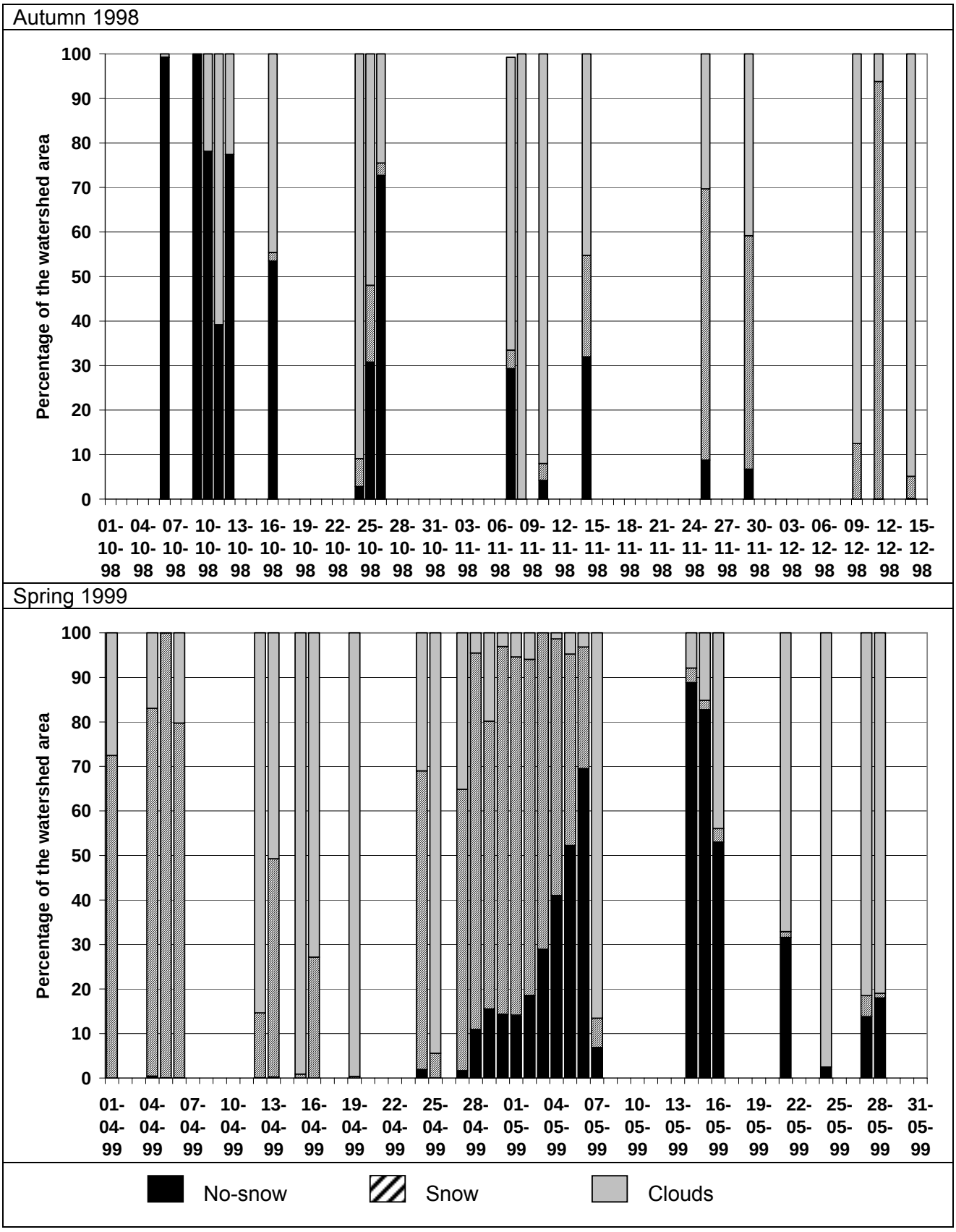

Figure 4: Classification results compiled over the Lac-Saint-Jean basin for the 1998-1999 period.

CONCLUSIONS

The objective of this work was to develop a simple procedure of space-time monitoring of snow cover over the province of Quebec using AVHRR images. The classification algorithm used herein was inspired by published classification techniques. This algorithm is based on sequential hierarchical thresholds in order to classify the AVHRR images into three surface categories: snow, no-snow and clouds. They were established empirically and they are consequently specific to the Quebec conditions. The algorithm was calibrated and validated over three winter seasons: 1998-1999, 1991-1992 and 1986-1987. The classification results were validated at the temporal and spatial levels using ground observations.

Compared to snow occurrence observations on ground, the algorithm correctly identifies snow/no-snow-covered pixels with a total precision of 87%. The algorithm permits to detect the presence of snow with an average precision of 90% and surfaces without snow with an average precision of 82%. It should be noted that the performances of the algorithm in spring and autumn are comparable. Also, the algorithm detects the presence of snow in open areas with a higher accuracy than in forest. In addition, the algorithm makes it possible to locate the beginning of the periods of formation and snow melt at the basin scale particularly under clear sky conditions. Also, the results showed that it is possible to seize the climatic differences between the three studied periods according to differences in the duration of winter seasons. It enables the inter-annual dynamics and the spatial variations in the establishment and the disappearance of snow cover to be seized as well. Therefore, the results show that the procedure developed in this work represents a suitable tool for the space-time monitoring of snow cover.

Furthermore, the application of the developed procedure was often limited by the presence of persistent cloud cover. In order to increase the size of the territory under cloud-free conditions, we will explore the potential of weekly composite snow cover extent maps made up of daily classified AVHRR images. We will also apply a procedure to merge the snow cover extent maps obtained using AVHRR data with those obtained using the passive microwave sensor SSM/I. This procedure will permit to combine the high spatial AVHRR resolution with the capacity of the SSM/I sensor to penetrate clouds.

ACKNOWLEDGEMENTS

The authors would like to thank Mrs. Veronique Beaulieu, undergraduate trainee, and Mr. Marc Philippin, research assistant, for their contributions. This study could not be carried out without the financial support of the consortium OURANOS and the NSERCC (ORC program).

REFERENCES

1 Caya D, R Laprise, M Giguère, G Bergeron, J P Blanchet, B J Stocks, G J Boer & N A McFarlane, 1995. Description of the Canadian regional climate model. Water, Air and Soil Pollution, 82: 477-482

2 Bitner D, T Carroll, D Cline & P Romanov, 2002. An assessment of the differences between three satellite snow cover mapping techniques. Hydrological Processes, 16: 3723-3733

3 Simic A, R Fernandes, R Brown, P Romanov & W Park, 2004. Validation of VEGETATION, MODIS, and GOES+SSM/I snow cover products over Canada based on surface snow depth observations. Hydrological Processes, 18: 1089-1104

4 Ramsay B H, 1998. The interactive multisensor snow and ice mapping system. Hydrological Processes, 12: 1537-1546

5 Hall D K, G A Riggs, V V Salomonson, N E DiGirolamo & K J Bayr, 2002. MODIS snow-cover products. Remote Sensing of Environment, 83: 181-194

6 Cracknell A P, 1997. The Advanced Very High Resolution Radiometer (AVHRR) (Taylor & Francis, London)

7 Rao C R N & J Chen, 1996. Post-launch calibration of the visible and near-infrared channels of the Advanced Very High Resolution Radiometer on the NOAA-14 spacecraft. International Journal of Remote Sensing, 17: 2743-2747

8 Qobilov T, F Pertziger, L Vasilina & M F Baumgartner, 2001. Operational technology for snow-cover mapping in the Central Asian mountains using NOAA-AVHRR data. IAHS-AISH Publication, 267: 76-80

9 Welch R M, N Rangaraj, M S Navar, S K Sengupta, A K Goroch & P Rabindra, 1992. Polar cloud and surface classification using AVHRR imagery: an intercomparison of methods. Journal of Applied Meteorology, 31: 405-420

10 Simpson J J, J R Stitt & M Sienko, 1998. Improved estimates of the areal extent of snow cover from AVHRR data. Journal of Hydrology, 204: 1-23

11 Fortin J P, M Bernier, A El Battay & Y Gauthier, 2000. Estimation of surface variables at the sub-pixel level for use as input to climate and hydrological models. In: Vegetation 2000, Belgirate, 3-6 April 2000, Italy (CNES, France)

12 Hall D K, G A Riggs, V V Salomonson & G R Scherfen, 2001. Earth Observing System (EOS) Moderate Imaging Spectroradiometer (MODIS) global snow-cover maps. IAHS-AISH Publication, 267: 55-60

13 Hutchison K D & J K Locke, 1997. Snow cover identification through cirrus-cloudy atmospheres using daytime AVHRR imagery. Geophysical Research Letters, 24: 1791-1794

14 Ananasso C, R Santoler, S Ma rullo & F D'Ortenzio, 2003. Remote sensing of cloud cover in the Arctic region from AVHRR data during the ARTIST experiment. International Journal of Remote Sensing, 24: 437-456

15 Voigt S, M Koch & M F Baumgartner, 1999. A multichannel threshold technique for NOAA AVHRR data to monitor the extent of snow cover in the Swiss Alps. IAHS-AISH Publication, 256: 35-43

16 Kangas M, M Heikinheimo & V Laine, 2001. Accuracy of NOAA AVHRR-based surface reflectance over winter-time boreal surface - comparison with aircraft measurements and land-cover information. Theoretical and Applied Climatology, 70: 231-244

17 Romanov P, G Gutman & I Csisar, 2000. Automated monitoring of snow cover over North America with multispectral satellite data. Journal of Applied Meteorology, 39: 1866-1880

18 Appel F& H Bach, 2003. Near-real-time derivation of snow cover maps for hydrological modeling using operational remote sensing data. In: IEEE IGARSS '03. Toulouse, France

19 Cihlar J & J Beaubien, 1998. Land Cover of Canada Version 1.1. Special Publication, NBIOME Project. Available on CD-ROM (Canada Centre for Remote Sensing & Canadian Forest Service, Natural Resources Canada, Ottawa, Ontario, Canada) 171-183
ftp://ftp2.ccrs.nrcan.gc.ca/ftp/ad/EMS/landcover95/

20 Tait A, Barton JS, Hall DK, 2001. A prototype MODIS-SSM/I snow-mapping algorithm. International Journal of Remote Sensing, 22: 3275-3284

21 Vikhamar D & R Solberg, 2002. Subpixel mapping of snow cover in forests by optical remote sensing. Remote Sensing of Environment, 84: 69-82

22 Barton J S, D K Hall & G A Riggs, 2000. Remote sensing fractional snow cover using Moderate Resolution Imaging Spectroradiometer (MODIS) data. In: 57th Eastern Snow Conference, edited by J Hardy (Syracuse, New York, USA) 171-183